

Quantum states and optics in a p -type heterojunction with lateral surface quantum dot or antidot superlattice subjected to perpendicular magnetic field

V.Ya. Demikhovskii * and D.V. Khomitsky
Nizhny Novgorod State University
Gagarin Ave. 23, Nizhny Novgorod 603950, Russia

The studies of quantum states and optics in a p -type heterojunction with lateral surface quantum dot (antidot) superlattice and in the presence of perpendicular magnetic field are performed. For the first time the Azbel'-Hofstadter problem is solved for holes in a complicated valence band described by the 4×4 Luttinger Hamiltonian. The set of magnetic subbands is obtained for separate hole levels in a wide interval of magnetic field. We found remarkable differences between hole spectra and the Hofstadter "butterfly" for electrons. The influence of the spin-orbit interaction onto wavefunctions and energy spectrum has been investigated. The probabilities of optical transitions between quantum states in the valence band and donors located in the monolayer inside the heterojunction are calculated. The set of parameters (superlattice periods, amplitude of periodic potential, magnitude of magnetic field, etc.) required for experimental observation of splitted hole Landau levels is determined.

PACS number(s): 73.21.-b, 73.21 Cd, 78.67.-n

I. INTRODUCTION

The problem of quantum states of 2D Bloch electrons subjected to magnetic field remains actual over several last decades. The fascinating physical phenomena occurring here are caused by the mutual effects of the crystalline periodic potential and the non-periodic vector potential of uniform magnetic field. The former leads to the energy band structure while the latter tends to form discrete energy levels. The crucial parameter determining the nature of quantum states in this problem is magnetic flux Φ penetrating the lattice elementary cell. If the flux is equal to rational number p/q of flux quanta $\Phi_0 = 2\pi\hbar c/|e|$ where p and q are mutually prime integers, it is possible to define a new set of translations on the lattice, called magnetic translations^{1,2} for which the quasimomentum is a good quantum number. To be specific, let the vector potential of uniform magnetic field B be chosen in Landau gauge

$$\mathbf{A} = (0, Bx, 0) \quad (1)$$

and $\Phi/\Phi_0 = p/q$. Under such conditions the simplest form of magnetic translations on a square lattice with the period a is

$$x \rightarrow x + qna, \quad y \rightarrow y + ma \quad (2)$$

where n and m are integers. From (2) it follows that an elementary cell in the presence of magnetic field (now called a magnetic cell) is q times larger in x direction, and the corresponding magnetic Brillouin zone (MBZ) is defined as

$$-\pi/qa \leq k_x \leq \pi/qa, \quad -\pi/a \leq k_y \leq \pi/a. \quad (3)$$

*demi@phys.unn.ru

The electron wavefunction gains an additional phase under the magnetic translations. The relation between the translated and the initial wavefunctions in magnetic field is known as the generalized Bloch conditions (or Peierls conditions)^{3,2}

$$\begin{aligned} \psi_{k_x k_y}(x, y, z) = & \psi_{k_x k_y}(x + qa, y + a, z) \exp(-ik_x qa) \times \\ & \times \exp(-ik_y a) \exp(-2\pi i p y/a). \end{aligned} \quad (4)$$

When the amplitude of periodic potential V_0 is smaller than the cyclotron energy $\hbar\omega_c$ one can neglect the influence of neighboring Landau levels and may obtain the set of magnetic subbands arising from a single level⁴. Although the magnitude of magnetic field is represented in terms of fraction p/q everywhere in the discussed theory, it should be stressed that the numerator p and the denominator q also exhibit themselves separately. In particular, every Landau level splits into p subbands with degeneracy degree q which means that the number of subbands depends only on p and the size of magnetic Brillouin zone (3) is a function only of q . If it becomes needful to include the interaction between Landau levels, numerical methods are usually applied^{5,7,8}. However, all dependencies on p , q , and p/q which have been mentioned in this paragraph, remain the same.

During last years several significant theoretical and experimental aspects of the discussed problem have been investigated. In particular, quantization of Hall conductance in 2D electron gas with additional periodic potential has been studied^{4,6,7,9,10}. One might expect that each of magnetic subbands gives a Hall conductance equal to e^2/ph , but according to Laughlin each subband must carry an integer multiple of the Hall current carried by the entire Landau level. In more complicated models describing Bloch electrons in magnetic field the manifestation of quantum chaos has been discovered¹¹⁻¹³.

Recently the number of experimental studies have been performed in order to investigate the electron quantum states in 2D heterojunctions with lateral surface superlattice of quantum dots (antidots). Such a system is convenient for investigation of both classical effects (commensurability of the lattice periods and cyclotron radius, transition to chaos, etc.) and of the energy spectrum consisting of magnetic subbands. For example, in Refs. 11,14 the oscillations of longitudinal magnetoresistance have been detected under the conditions where classical cyclotron radius $2R_c$ envelopes an integer number of antidots or numerous reflections from one antidot occur. The first experimental evidences of Landau levels splitted into the set of magnetic subbands have been obtained by longitudinal magnetoresistance studies¹⁵. Then, the measurements of Hall resistance in a subband energy spectrum of 2D electrons have also been performed¹⁶. In several recent publications the magnetotransport in 2D hole gas with lateral periodic modulation was studied^{17,18}.

Besides the magnetotransport measurements, the attempts of magneto-optical studies of inter-band transitions between the conduction band and acceptor impurities have been performed in n -type heterostructures¹⁹. The experiments in p -type heterojunctions without periodic potential have also become possible due to the progress in technology which substantially improved the quality of p channels in GaAs/AlGaAs heterojunctions²⁰. Thus, almost all intriguing phenomena found for 2D electron systems were also observed in 2D hole channels.

The specific features of hole quantum states which have caused the interest to them may be briefly described as non-trivial effects of symmetry and the spin-orbit interaction. It is known that in the absence of magnetic field the electron spectrum in a symmetrical quantum well is twofold degenerate with respect to spin. Opposite, in an asymmetrical heterojunction grown, for example, in z direction where $V(z) \neq V(-z)$ the relativistic orbital interaction of the electron magnetic moment and macroscopic heterojunction potential leads to the breakdown of spin degeneracy. Only twofold Kramers degeneracy $E(\mathbf{k}, \uparrow) = E(-\mathbf{k}, \downarrow)$ remains. In order to obtain transparent and valuable results from transport and optical experiments, one may need to choose the set of parameters (superlattice periods, value of magnetic field and amplitude of periodic potential, etc.) which provide a sharp, easily distinguishable picture of non-overlapped magnetic subbands originating from a particular Landau level. Such energy spectra and wavefunctions are studied in the present paper together with calculation of luminescence intensities for transitions between magnetic subbands and impurities. In Sec. II we study the hole quantum states in a p -type heterojunction subjected to magnetic field only (Subsec. II A) and both to magnetic field and the periodic potential of quantum dot superlattice (Subsec. II B). The spin-orbit coupling is included here which is principal for

the description of holes in semiconductors. For the first time the calculation of magnetic subbands and four-component wavefunctions for holes in a heterojunction is performed. It was found that the structure of hole magnetic subbands differs from the well-known Hofstadter "butterfly", especially at high magnetic field. Then in Sec. III we calculate the matrix elements and luminescence intensities for direct optical transitions between hole magnetic subbands and electrons bound to donors which are located in the monolayer inside the heterojunction. The huge difference in the magnitude of luminescence intensities corresponding to different magnetic subbands was found and the dependence of transition probabilities on polarization was investigated. These results may be used for identification of complicated magnetic subband spectra in magneto-optical experiments. The summary of our results is given in Sec. IV.

II. HOLE QUANTUM STATES IN THE PRESENCE OF LATERAL SUPERLATTICE AND MAGNETIC FIELD

A. Hole Landau levels in a p -type heterojunction without periodic potential

Let us now consider the upper edge of GaAs p -like valence band near the Γ_8 -point $\mathbf{k} = 0$. In the presence of the external magnetic field \mathbf{B} in the $\langle 001 \rangle$ direction (hereafter denoted by z), the effective Hamiltonian H_L (neglecting linear k terms) is obtained from the 4×4 Luttinger Hamiltonian^{21,22} by replacing the components of the wave vector by their operator forms,

$$k_\alpha \rightarrow \hat{k}_\alpha = -i \frac{\partial}{\partial x_\alpha} + \frac{e}{c} A_\alpha. \quad (5)$$

Besides, one has to include the κ terms, which represent the interaction of the electron's spin magnetic moment with the external magnetic field. In this section the atomic units $\hbar = m_0 = 1$ are used. Writing H_L in terms of the creation and destruction operators,

$$a^+ = \frac{R_c}{\sqrt{2}} k_+, \quad a = \frac{R_c}{\sqrt{2}} k_- \quad (6)$$

where $k_\pm = k_x \pm ik_y$, $R_c = [\frac{c}{eB}]^{1/2}$, and making the no-warping approximation, one obtains the H_L in the following form:

$$H_L = \begin{bmatrix} H_{11} & \bar{\gamma}\sqrt{3}(eB/c)a^2 & \gamma_3\sqrt{6eB/c}k_z a & 0 \\ & H_{22} & 0 & -\gamma_3\sqrt{6eB/c}k_z a \\ & & H_{33} & \bar{\gamma}\sqrt{3}(eB/c)a^2 \\ & & & H_{44} \end{bmatrix}, \quad (7)$$

where

$$\begin{aligned} H_{11} &= -(\gamma_1/2 - \gamma_2)k_z^2 - (eB/c) \left[(\gamma_1 + \gamma_2) \left(a^+ a + \frac{1}{2} \right) + \frac{3}{2} \kappa \right], \\ H_{22} &= -(\gamma_1/2 + \gamma_2)k_z^2 - (eB/c) \left[(\gamma_1 - \gamma_2) \left(a^+ a + \frac{1}{2} \right) - \frac{1}{2} \kappa \right], \\ H_{33} &= -(\gamma_1/2 + \gamma_2)k_z^2 - (eB/c) \left[(\gamma_1 - \gamma_2) \left(a^+ a + \frac{1}{2} \right) + \frac{1}{2} \kappa \right], \\ H_{44} &= -(\gamma_1/2 - \gamma_2)k_z^2 - (eB/c) \left[(\gamma_1 + \gamma_2) \left(a^+ a + \frac{1}{2} \right) - \frac{3}{2} \kappa \right]. \end{aligned}$$

The lower half of matrix (7) is obtained by Hermitian conjugation. The hole energy here is measured as negative, e is a modulus of elementary charge, $\bar{\gamma} = (\gamma_2 + \gamma_3)/2$. The band parameters appearing in (7) are taken from Ref.22: $\gamma_1 = 6.85$, $\gamma_2 = 2.1$, $\gamma_3 = 2.9$, and $\kappa = 1.2$. The Luttinger

Hamiltonian (7) is written in a basis of p -like atomic functions $v_j(\mathbf{r})$ which transform as a set of eigenfunctions of the angular momentum operator $J = 3/2$. These $|J; m_J\rangle$ basis functions may be written as following:

$$\begin{cases} v_1 = |\frac{3}{2}; \frac{3}{2}\rangle = |-\sqrt{1/2}(x + iy) \uparrow\rangle, \\ v_2 = |\frac{3}{2}; -\frac{1}{2}\rangle = |-\sqrt{1/6}(x - iy) \uparrow - \sqrt{2/3}z \downarrow\rangle, \\ v_3 = |\frac{3}{2}; \frac{1}{2}\rangle = |\sqrt{1/6}(x + iy) \downarrow - \sqrt{2/3}z \uparrow\rangle, \\ v_4 = |\frac{3}{2}; -\frac{3}{2}\rangle = |-\sqrt{1/2}(x - iy) \downarrow\rangle, \end{cases} \quad (8)$$

where the arrows indicate the z -projection of spin. The holes in GaAs/AlGaAs p -type heterojunction grown in z direction which is parallel to the magnetic field are confined by the smoothly varying potential $V_h(z)$ which allows us to apply the effective-mass approximation. The potential $V_h(z)$ is of a triangular shape, and on the boundary $\psi(0) = 0$. It should be noted that such a shape does not have the inversion symmetry, i.e. $V_h(z) \neq V_h(-z)$ which leads to the breakdown of the twofold spin degeneracy and to the splitting of energy levels of the effective-mass Hamiltonian

$$H_{eff} = H_L(a^+, a, k_z) + V_h(z) \cdot \hat{E} \quad (9)$$

even at the absence of magnetic field²². Hereafter \hat{E} stands for a unit 4×4 matrix. The lack of inversion symmetry of the atomic potential of GaAs crystal lattice is present also in bulk material and is described by linear k -terms in Luttinger Hamiltonian. However, the effects caused by these terms (the displacement of subband maximum in \mathbf{k} -space^{23,24}) are negligible compared with those induced by heterostructure potential and thus are not considered here.

We first observe that for $B = 0$ the Hamiltonian (9) becomes diagonal with elements

$$\begin{aligned} H_h &= -(\gamma_1/2 - \gamma_2) \frac{d^2}{dz^2} + V_h(z), \\ H_l &= -(\gamma_1/2 + \gamma_2) \frac{d^2}{dz^2} + V_h(z) \end{aligned}$$

that yields an infinite set of doubly degenerate heavy and light hole subband energies and eigenfunctions $c_{\nu_j}(z)$, $\nu = 1, 2, \dots$. These functions are usually obtained by solving Schrödinger and Poisson equations self-consistently. As a result, the shape of potential $V(z)$ has a varying gradient which reflects the changes in electric field inside the heterojunction^{20,22}. Thus, the precise shape of functions $c_{\nu_j}(z)$ differs from the one for the case of uniform electric field. However, the investigations of energy spectrum and the matrix elements of transitions between 2D Bloch quantum states and impurities require only the information about the overlapping between different localized functions $c_{\nu_j}(z)$, and between them and well-known wavefunctions of impurities. The intervals of localization for $c_{\nu_j}(z)$ can be obtained with high accuracy for all subbands of size quantization considered in this paper since the shape of $V(z)$ in a single GaAs/AlGaAs heterojunction is well-known²². The solution of the effective-mass equation with the Hamiltonian (9) may be written as a four-component vector of envelope functions in the $|J; m_J\rangle$ basis (8). As it was shown by Luttinger²¹, in the presence of magnetic field and under axial approximation one can distinguish the eigenstates of operator (9) by a discrete quantum number N which defines the particular set of Landau quantum states. These states have k_y -component of momentum under Landau gauge (1). In the presence of the heterostructure potential the k_z -component in (9) is replaced by the operator $k_z = -i\partial/\partial z$. Hence, an eigenstate F_{Nk_y} of the operator (9) consists of four envelope functions and the hole wavefunction is written as

$$\Psi_{Nk_y} = \sum_{j=1}^4 F_{jNk_y} v_j \quad (10)$$

where v_j is a $|J; m_J\rangle$ basis function and

$$F_{Nk_y} = e^{ik_y} (C_1(z)u_{N-2}, C_2(z)u_N, C_3(z)u_{N-1}, C_4(z)u_{N+1}). \quad (11)$$

In Eq.(11) $u_N(x)$ is a harmonic oscillator wavefunction and the envelope functions $C_j(z)$ are constructed as a superposition of the zero-field functions $c_{\nu_j}(z)$ with numerically defined coefficients, which vanish for negative indexes N . For example, for $N = -1$ one can obtain $F_{-1} = (0, 0, 0, C_4(z)u_0)$, for $N = 0$ the solution $F_0 = (0, C_2(z)u_0, 0, C_4(z)u_1)$, and for $N \geq 2$ all four components of (11) will be nonzero²⁵. After substituting the function (11) into the Schrödinger equation with the Hamiltonian (9) one obtains an algebraic eigenvalue problem. We restrict ourselves to the first three levels of size quantization which corresponds to two heavy- and one light-hole levels. This approximation seems to be valid in heterojunctions with typical hole concentration $n_h = 5 \times 10^{11} \text{cm}^{-2}$ and depletion-layer density $N_{dep} = 10^{15} \text{cm}^{-3}$ for which only the lowest hole level is occupied^{22,20}. For each level of size quantization we take into account several Landau levels shown on Fig.1. Here one can see the electron-like behavior of light-hole Landau levels at low magnetic field caused by proximity of the second heavy-hole subband. We assume that the introduction of periodic potential with the amplitude V_0 (see the following Subsec.) does not change $c_{\nu_j}(z)$ significantly since $|V_0|$ considered in our paper is much smaller than the size quantization energies. Hence, in our further studies we use the matrix elements of the effective Hamiltonian (9) calculated for the functions $c_{\nu_j}(z)$ and the size quantization energies which have been discussed above.

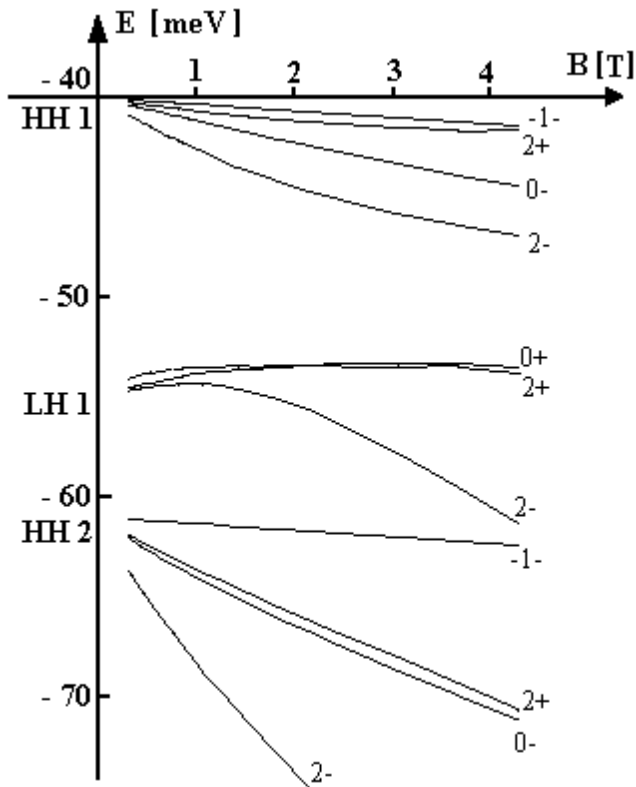


FIG. 1. Set of hole Landau levels corresponding to the first three subbands of size quantization (two heavy-hole levels HH1, HH2, and one light-hole level LH1). The electron-like behavior of the light-hole Landau levels at low magnetic field can be observed. Each level is characterized by Landau index $N = -1, 0, 1, \dots$ and by dominating spin projection \pm (see text). Hereafter the energy is measured from the top of the valence band in bulk GaAs.

B. Bloch quantum states in the presence of lateral surface superlattice

The problem of hole quantum states in a p -type heterojunction subjected to magnetic field and affected by a lateral superlattice is described by the Schrödinger equation with the vector potential (1) and the 2D periodic potential of a lateral superlattice which can be chosen in the form⁸

$$V(x, y) = V_0 \cos^2 \frac{\pi x}{a} \cos^2 \frac{\pi y}{a}. \quad (12)$$

Here a is the superlattice period and the case $V_0 < 0$ (> 0) corresponds to the periodic electric potential generated by quantum dot (antidot) superlattice. The Hamiltonian for magnetic Bloch hole quantum states is a sum of (9) and (12):

$$H = H_{eff} + V(x, y) \cdot \hat{E}, \quad (13)$$

The eigenvectors of the operator (13) are four-component envelope functions written in the $|J; m_J\rangle$ basis (8):

$$\Psi_{k_x k_y}^{envelope}(\mathbf{r}) = \left(\psi_{k_x k_y}^{(1)}(\mathbf{r}), \psi_{k_x k_y}^{(2)}(\mathbf{r}), \psi_{k_x k_y}^{(3)}(\mathbf{r}), \psi_{k_x k_y}^{(4)}(\mathbf{r}) \right), \quad (14)$$

and the total hole wavefunction is

$$\begin{aligned} \Psi_{k_x, k_y}(\mathbf{r}) = & \psi_{k_x k_y}^{(1)}(\mathbf{r}) \left| \frac{3}{2}; \frac{3}{2} \right\rangle + \psi_{k_x k_y}^{(2)}(\mathbf{r}) \left| \frac{3}{2}; -\frac{1}{2} \right\rangle + \\ & \psi_{k_x k_y}^{(3)}(\mathbf{r}) \left| \frac{3}{2}; \frac{1}{2} \right\rangle + \psi_{k_x k_y}^{(4)}(\mathbf{r}) \left| \frac{3}{2}; -\frac{3}{2} \right\rangle. \end{aligned} \quad (15)$$

The crucial statement here is the following: as long as the periodic potential (12) is applied, every hole envelope function in Eq.(14) becomes a magnetic Bloch function classified by k_x and k_y quantum numbers varying in the MBZ (3). It should be mentioned that the translation properties of each component of the envelope function (14) in (xy) plane are the same as for the single-component electron wavefunction. In particular, every component of (14) satisfies to the Peierls condition (4). Hence, one can write the components of (14) as a superposition of the Landau quantum states as it was demonstrated in Refs.4,8, namely

$$\begin{aligned} \psi_{k_x k_y}^{(j)}(\mathbf{r}) = & \frac{1}{La\sqrt{q}} \sum_{\nu_j} c_{\nu_j}(z) \sum_{N_j} \sum_{n=1}^p G_{j\nu_j N_j n}(k_x, k_y) \sum_{l=-L/2}^{L/2} u_{N_j} \left(\frac{x - x_0 - lqa - nqa/p}{\ell_H} \right) \times \\ & \times \exp \left(ik_x \left[lqa + \frac{nqa}{p} \right] \right) \exp \left(2\pi iy \frac{lp + n}{a} \right) \exp(ik_y y), \end{aligned} \quad (16)$$

where for a particular $|J; m_J\rangle$ projection j we take into account several levels of size quantization ν_j and for each of them we assume several Landau levels N_j . Then, analogous to the electron problem described, for example, in Refs 5-7,9, after substituting the wavefunction (15) into the Schrödinger equation with the Hamiltonian (13) one obtains the eigenvalue problem for the coefficients $G_{j\nu_j N_j n}(k_x, k_y)$ and the hole magnetic subbands $\varepsilon_{\nu_j N_j n}(k_x, k_y)$:

$$\sum_{j'\nu'_j N'_j n'} \left(H_{j\nu_j N_j n}^{j'\nu'_j N'_j n'} + V_{j\nu_j N_j n}^{j'\nu'_j N'_j n'}(p/q, k_x, k_y) \right) G_{j'\nu'_j N'_j n'} = \varepsilon G_{j\nu_j N_j n}. \quad (17)$$

Here the notation $H_{j\nu_j N_j n}^{j'\nu'_j N'_j n'}$ is used for the projection of the Hamiltonian (9) onto our basis $(j \nu_j N_j n)$ and $V_{j\nu_j N_j n}^{j'\nu'_j N'_j n'}(p/q, k_x, k_y)$ stands for the matrix elements of the periodic potential (12) calculated in this basis. We have diagonalized the system (17) for different values of magnetic field

and different amplitudes of periodic potential. The maximum size of Hermitian matrix in (17) was up to 220×220 . The corresponding energy spectra and hole wavefunctions are shown on Figures 2 – 6.

It was mentioned previously that hole Landau levels may be classified into groups of the effective Hamiltonian (13) eigenvalues labeled by the common index $N = -1, 0, 1, \dots$. For example, for $N = 0$ such a group belonging to the subband of size quantization with $\nu = 1$ consists of one heavy- and one light-hole level. These levels can be obtained by the diagonalization of 2×2 matrix and are labeled by $N = 0 - (+)$ (see Fig.1). When the periodic potential of lateral superlattice is introduced, the 2×2 matrix yields $2p \times 2p$ matrix equation (17) which spectrum consists of $2p$ magnetic subbands originating from $N = 0 - (+)$ levels. If the amplitude $|V_0|$ is small enough to neglect the influence of other levels neighboring with the levels $N = 0 - (+)$, it is possible to study their splitting separately. The set of $2p$ magnetic subbands originating from the levels $N = 0 - (+)$ splitted by the periodic potential with $V_0 = -3meV$ is shown on Fig.2a(b) versus the reciprocal magnetic flux q/p . Comparing Fig.2 and the ordinary Hofstadter "butterfly" for 2D electrons, one can see that at low magnetic field $q/p \approx 1$ the hole spectrum looks similar to the electron one, in particular, the clustering of hole magnetic subbands is the same. At high magnetic fields $q/p \ll 1$ one can see the down and up shifts of the energy on Fig.2 with respect to the center of the "butterfly" at $q/p \approx 1$. This difference between hole and electron spectra is caused

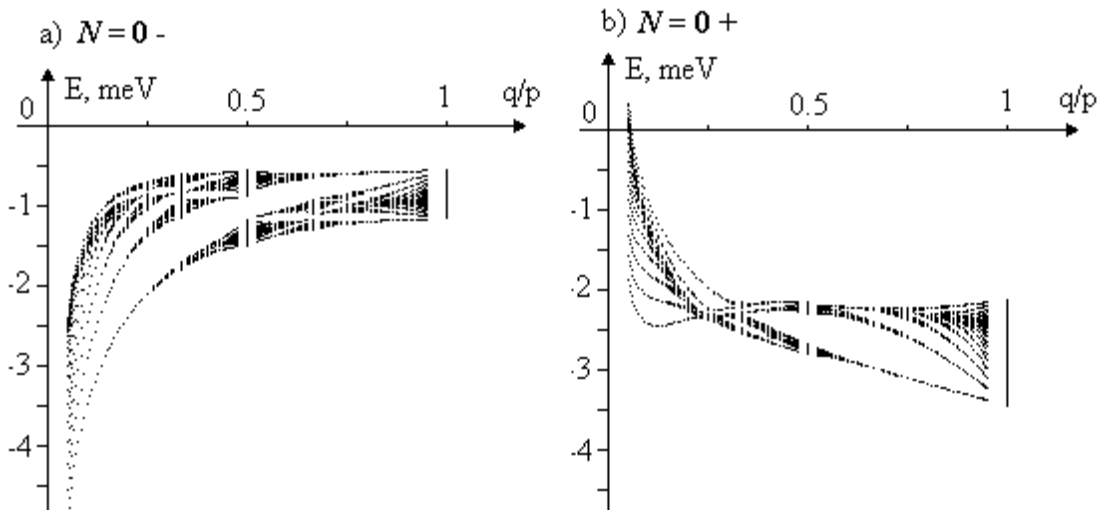


FIG. 2. Energy spectrum of 2D hole gas laterally modulated by the quantum dot superlattice with $a = 80nm$ plotted vs reciprocal magnetic flux q/p . The spectrum is shown for two hole levels $N = 0 - (+)$ coupled by the off-diagonal term of the Luttinger Hamiltonian and splitted by periodic potential (12) with the amplitude $V_0 = -3meV$.

Hereafter we are going to be interested mainly in the hole energy spectra at high (and fixed) magnetic field $p/q = 20$ which corresponds to $B \approx 12$ T. The spectrum of system (17) for such magnetic flux and for $k_x = k_y = 0$ is shown on the bottom part of Fig.3 for the case of non-overlapped subbands related to the highest hole levels $N = 2+$ and $N = -1-$. Here the sign $+(-)$ refers to the spin projection of the dominating component of $|J; m_J\rangle$ basis^{22,20}. Similar to the electron spectra^{6,8}, every hole Landau level has splitted into p narrow magnetic subbands (which look like discrete levels) grouped near the unperturbed Landau level (marked as a dark circle on Fig.3). Note that the $N = 2+$ and $N = -1-$ levels on Fig.3 have exchanged their positions in energy with respect to Fig.1 which is due to the level crossing occurred at some intermediate p/q . The condition $|V_0| \leq \Delta E_{12}$ where ΔE_{12} is the distance between the levels $N = 2+$ and $N = -1-$ allows to observe the set of non-overlapped magnetic subbands for these levels at high magnetic

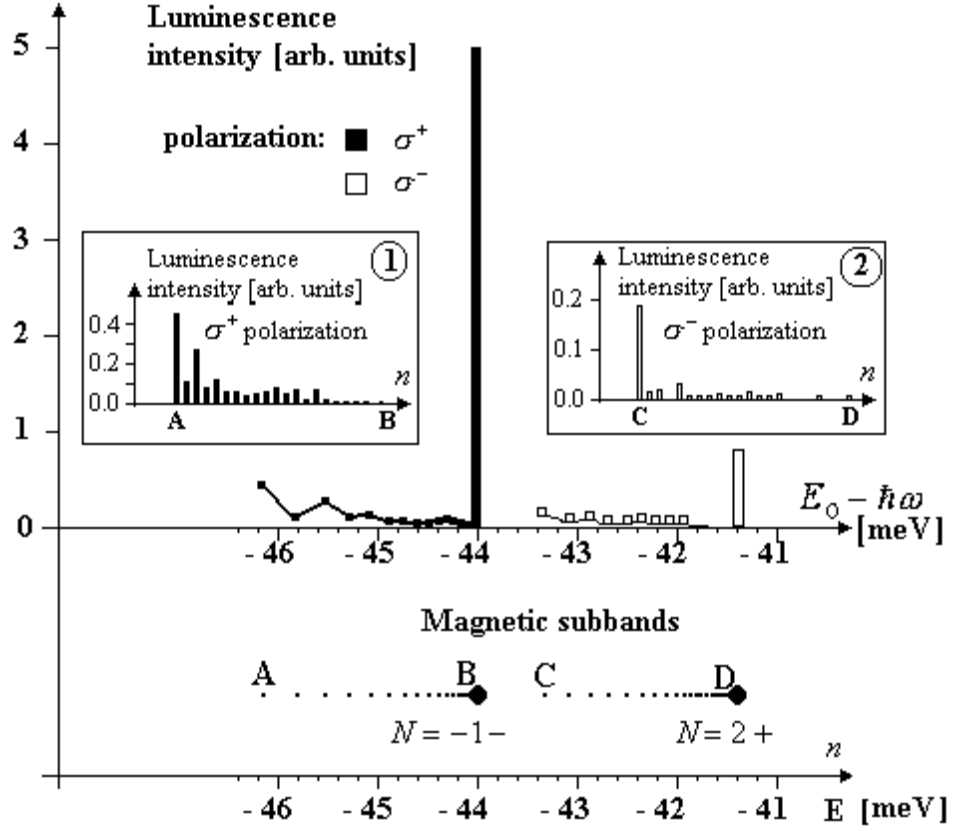


FIG. 3. (Bottom) non-overlapped hole magnetic subbands related to the highest Landau levels $N = 2+$ and $N = -1-$ (black circles) at $p/q = 20$ splitted by the periodic potential of quantum dot superlattice with the amplitude $V_0 = -2.5\text{meV}$. (Top) intensities of the luminescence with σ^+ (black) and σ^- (white) polarization for transitions between donor levels and hole subbands plotted vs. the photon energy $\hbar\omega$ together with the intensities of transitions to the unperturbed ($V_0 = 0$) hole levels. The latter are shown as single bars above the level positions. The insets 1 and 2 show the fine structure of the transition intensities with respect to subband number, and the donor energy E_0 is counted from the Γ_8 point of GaAs valence band.

In the following Sec. we will calculate the matrix elements for transitions between the valence band and donors located in the heterojunction and thus the knowledge of hole wavefunction in a superlattice cell is required. On Fig.4a,b we plot the $Re\psi_j > 0$ (top) and the $|\psi_j|^2$ (bottom) for the hole wavefunction component $m_J = -3/2$ at $k_x = k_y = 0$ for subbands A and B which are indicated on Fig.3. We've not shown the contour plots for the imaginary part of the wavefunction since they demonstrate qualitatively the same behavior. It should be noted that for subbands located between A and B (including themselves) the other $|J; m_J\rangle$ components in (15) are negligible under the conditions of a non-overlap with other subbands. This is a consequence of a single-component structure of the eigenvector $F_{-1} = (0, 0, 0, C_4(z)u_0)$ corresponding to the $N = -1$ Landau level shown on Fig.1. The impact of other components in our model can be provided only by the external periodic potential $V(x, y)$ leading to the Landau level coupling, but this coupling is negligible for the non-overlapped subbands shown of Fig.3, and thus no other $|J; m_J\rangle$ components are present on Fig.4. As for the single-component electron quantum states⁸, $Re\psi_j$ (and $Im\psi_j$ also) have different structure with respect to the subband number n . Namely, in the subband A located far from the clustering point, the $Re\psi_j$ (upper part of Fig.4a) has much less oscillations than the $Re\psi_j$ for the subband B belonging to the clustering region (upper part of Fig. 4b). It should be noted that the probability density distribution (bottom parts of Fig.4a,b) is always smooth and square symmetric, despite the possible oscillatory character of $Re\psi_j$ or $Im\psi$. One can see that the probability density shown on bottom parts of Fig.4a,b always has the C_4 symmetry which corresponds to the symmetry of the superlattice, while $Re\psi_j$ can have lower symmetry (upper part of Fig.4b) because of the non-symmetrical Landau gauge (1). It can be expected that the discussed difference in the $Re\psi_j$ shape in differe

from donors an

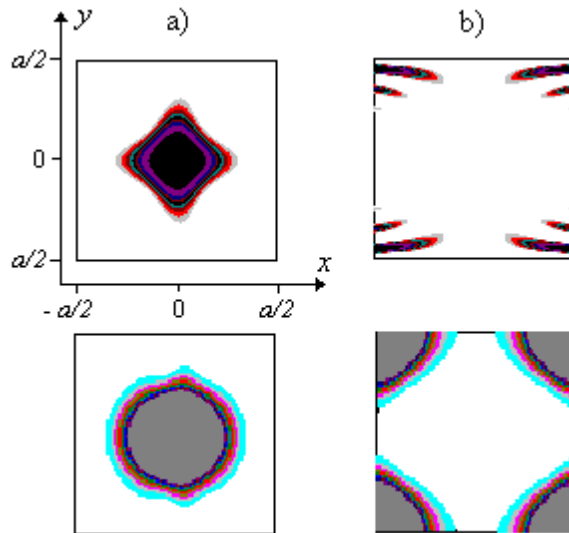


FIG. 4. Envelope hole wavefunctions $Re\psi_j > 0$ (top) and probability density distributions (bottom) for the component $m_J = -3/2$ plotted in one superlattice cell at $k_x = k_y = 0$ for subbands A (Fig.4a) and B (Fig.4b) shown on Fig.3.

When the condition $|V_0| < \Delta E_{12}$ is not fulfilled, the structure of hole spectrum looks different. The spectrum for $V_0 = -10meV$ and $\Delta E_{12} \approx 2.5meV$ is shown on the bottom part of Fig.5.

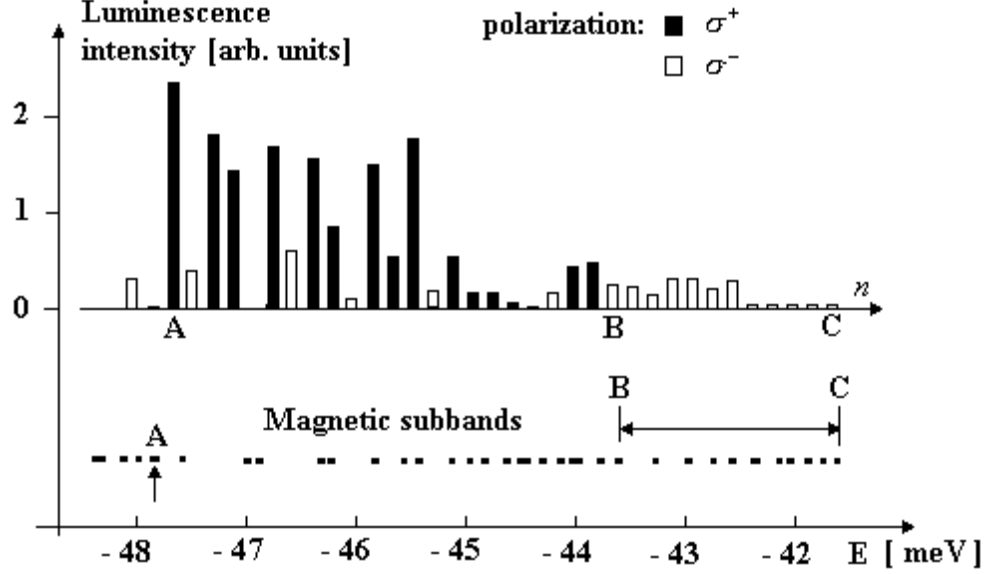


FIG. 5. (Bottom) overlapped hole magnetic subbands related to the same Landau levels but splitted by the periodic potential with larger amplitude $V_0 = -10meV$. (Top) intensities of the luminescence with σ^+ (black) and σ^- (white) polarization for transitions between the monolayer of donors and hole subbands plotted vs the subband number n .

In this case the magnetic subbands originating from different hole Landau levels are strongly overlapped almost everywhere except the region near the highest Landau level. This region is marked on Fig.5 and it contains magnetic subbands from B to C belonging to the Landau level $N = 2+$. In this interval of non-overlapping subbands one may expect a distinguishable behavior of transition intensities for these subbands (see the following Sec). Under the conditions of strong subbands overlap the domination of one of $|J; m_J\rangle$ basis component becomes less pronounced. This is illustrated on Fig.6 where we plot the probability distributions $|\psi_j|^2$ for all four $|J; m_J\rangle$ components of the wavefunction (15) in the subband A marked by an arrow on Fig.5. It is clearly seen that all the components have the same order which is a consequence of the overlapping between the magnetic subbands originating from Landau levels with different dominating wavefunction

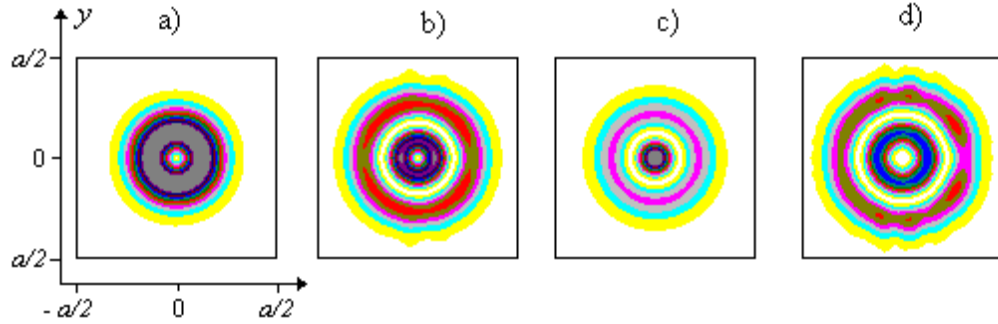


FIG. 6. Probability distribution $|\psi_j|^2$ of four hole wavefunction components at $k_x = k_y = 0$ for the subband A marked by an arrow on Fig.5. The figures (a) – (d) correspond to the components $|\frac{3}{2}; \frac{3}{2}\rangle$, $|\frac{3}{2}; -\frac{1}{2}\rangle$, $|\frac{3}{2}; \frac{1}{2}\rangle$ and $|\frac{3}{2}; -\frac{3}{2}\rangle$ of $|J; m_J\rangle$ basis, respectively.

III. LUMINESCENCE INTENSITIES FOR DONORS - VALENCE BAND TRANSITIONS

As it was mentioned in the Introduction, one of the experimental methods for investigation of quantum states in magnetic subbands is a magneto-optical measurement of transition intensities. Below we calculate the matrix elements and intensities of transitions between the electrons bound to the monolayer of shallow donors and the magnetic Bloch hole states in the valence band.

Let us consider a process in which photon is emitted and the electron is dropped from the donor atom to the valence band. Following Ref.20, we suppose that the monolayer of donors is located at a well-defined distance from the heterojunction interface. The final quantum state $\Psi_{k_x k_y}^f$ is the hole wavefunction (15), and the initial quantum state Ψ^i is a hydrogen-like wavefunction of a donor impurity located inside the heterojunction at the distance $z = z_0$ from the interface and at the point (x_0, y_0) in the superlattice cell. This impurity is described by the envelope function $\psi_D(\mathbf{r}, \mathbf{r}_0)$ where $\mathbf{r}_0 = (x_0, y_0, z_0)$ and

$$\psi_D(\mathbf{r}, \mathbf{r}_0) = A \exp\left(-\frac{1}{r_D} [(x - x_0)^2 + (y - y_0)^2 + (z - z_0)^2]^{1/2}\right),$$

where $r_D = \kappa_e \hbar^2 / m^* e^2$ stands for the donor Bohr radius in GaAs/AlGaAs heterostructure with the dielectric constant κ_e and the effective mass at the bottom of conduction band m^* . The value of r_D obtained from luminescence measurements is about 15 nm²⁰. The conduction band is characterized by an s -type atomic function $s_\alpha(\mathbf{r})$ where the index $\alpha = 1(2)$ corresponds to the function $|s \uparrow\rangle$ ($|s \downarrow\rangle$). Since the total ensemble of donor atoms does not have a definite projection of an angular momentum, one can write

$$\Psi^i = \psi_D(\mathbf{r}, \mathbf{r}_0) \cdot \frac{|s \uparrow\rangle + |s \downarrow\rangle}{\sqrt{2}}.$$

After the definition of initial and final quantum states one can write the magnetoluminescence intensity $I(\hbar\omega)$ as

$$I(\hbar\omega) \propto \sum_{if} \overline{|M_{if}|^2} \delta(E_f - E_i - \hbar\omega) \quad (18)$$

where we assume that the initial state Ψ^i is fully occupied and the final state $\Psi_{k_x k_y}^f$ is empty. If the energy of electrons bound to donors is fixed, the summation over the initial states in (18) reduces to the multiplication by the total number of donor atoms. The matrix element for transition between a donor and a hole state is²⁶

$$\begin{aligned} M_{if} &= \langle \Psi_{k_x k_y}^f | \mathbf{p} \cdot \mathbf{e} | \Psi^i \rangle = \\ &= \sum_{\alpha=1}^2 \sum_{j=1}^4 \langle v_j | \mathbf{p} \cdot \mathbf{e} | s_\alpha \rangle \langle \psi_{k_x k_y}^{(j)} | \psi_D \rangle + \sum_{\alpha=1}^2 \sum_{j=1}^4 \langle \psi_{k_x k_y}^{(j)} | \mathbf{p} \cdot \mathbf{e} | \psi_D \rangle \langle v_j | s_\alpha \rangle, \end{aligned} \quad (19)$$

where \mathbf{e} being a unit vector in the direction of electric field and the scalar products are defined as

$$\begin{aligned} \langle v_j | (\dots) | s_\alpha \rangle &= \int_{cell} v_j(\mathbf{r})^* (\dots) s_\alpha(\mathbf{r}) d\mathbf{r}, \\ \langle \psi_{k_x k_y}^{(j)} | (\dots) | \psi_D \rangle &= \int_{crystal} \psi_{k_x k_y}^{(j)*}(\mathbf{r}) (\dots) \psi_D(\mathbf{r}) d\mathbf{r}. \end{aligned}$$

The first term in (19) corresponds to the matrix elements of the transitions from donors to the valence band. The second term vanishes due to the orthogonality of the $|J; m_J\rangle$ functions $v_j(\mathbf{r})$ and $s_\alpha(\mathbf{r})$ being p - and s -type functions, respectively. It should be stressed that the transitions

from donors to hole subbands belonging to different Landau levels are characterized by different polarization. On the one hand, it is a consequence of different contribution of the $|J; m_J\rangle$ basis components into the hole quantum state (15) and, on the other hand, it is due to the fact that the transitions from heavy holes are three times more intensive than those from light holes (see, for example, Refs. 20,26). The overlapping of hole and donor wavefunctions and thus the matrix element strongly depend on the position of the donor atom in a current superlattice cell. In order to obtain the transition probability for a superlattice with many cells we have to average it over many possible donor positions in the (xy) plane, i.e.

$$\overline{|M|^2} = \frac{1}{N_D} \sum_{x_0 y_0} |M(x_0 y_0)|^2, \quad (20)$$

where N_D is the total number of donor positions. We found that due to the random position of a donor atom the matrix elements practically (with an accuracy of few percents) do not depend on the quasimomentum which classify the Bloch quantum state. This independence on k_x and k_y is stipulated by the fact that the radius of the donor wavefunction is considerably smaller than the superlattice period a . By taking this into account, the summation over the final states in (18) is also performed simply. The magnetic subbands are very narrow at $p/q = 20$ and their widths are apparently smaller than the collision broadening (the corresponding estimations for the electron gas can be found, for example, in Ref.6). So, one can treat the magnetic subbands at $p/q = 20$ as a set of levels with fixed energy and thus also replace the summation over the final states in (18) by multiplication by the total number of states in a magnetic subband. This number is determined by the area of the magnetic Brillouin zone (3) which is equal for all subbands. As a result, we found that the variations of intensity (18) with respect to the photon energy almost precisely repeat the behavior of matrix elements (20).

On the upper side of Fig.3 we show the results for the luminescence intensities with σ^+ and σ^- circular polarization calculated for two highest Landau levels $N = -1-$ and $N = 2+$ at $p/q = 20$ being splitted by the periodic potential (12) with the amplitude $V_0 = -2.5meV$. On the horizontal axis we plot the photon energy $\hbar\omega$ counted from the energy E_0 which is the distance between a donor level and the Γ_8 point of the valence band. In order to compare these values with the intensities of transitions to the unperturbed Landau levels ($V_0 = 0$) we plot these intensities on the right side of each histogram of Fig.3 directly above the position of the hole Landau levels. Qualitatively, the maximum intensity of transitions to one of p magnetic subbands is approximately p times smaller than for the non-splitted Landau level which corresponds to the ratio (equal to p) of the number of quantum states in one Landau level and in one magnetic subband. It is evident that the magnetic subbands related to different Landau levels provide the luminescence with different polarization, just like the unperturbed hole Landau levels²⁰. Namely, for σ^+ polarization only the transitions to magnetic subbands originating from $N = -1-$ level can be observed while for σ^- polarization the transitions to subbands from $N = 2+$ level are significant. On the insets 1,2 on Fig.3 we show in detail the dependence of the transition intensities on a subband number. One can see that the transitions to subbands located far from the clustering point (subbands A and C) are more intensive than for subbands near the unperturbed Landau levels (subbands B and D). Such a behavior is a consequence of the oscillatory character of hole wavefunctions in B - and D -type subbands (see Fig.4). Namely, the space scale of the wavefunction in subband A (Fig.4a) is of the same order as the lattice constant a (which is larger than the donor Bohr radius r_D) while the period of wavefunction oscillations on Fig.4b is considerably smaller than r_D . As a result, the matrix element for transitions in B -type subbands decreases rapidly which explains the sharp saturation (observable on the insets 1 and 2 on Fig.3) of transitions to B - and D -type subbands compared with A - and C -type. We believe that the described differences in magneto-optical parameters will provide more transparency in experimental studies of hole magnetic subbands.

The behavior of transition intensities changes drastically when $|V_0|$ is increased. As it was mentioned previously, the overlapping of magnetic subbands occur when $|V_0| > \Delta E_{12}$. The transition intensities for such a case are shown on the upper part of Fig.5 for the same Landau levels $N = -1-$ and $N = 2+$ at $p/q = 20$ splitted by the periodic potential of quantum dots (12) with

higher amplitude $V_0 = -10meV$. One can see that the switching of polarization from σ^+ to σ^- leads to the total decrease of transition intensities but their dependence on n changes significantly mainly for subbands $B - C$ which are not overlapped with those related to other Landau levels (see the marked region on the bottom part of Fig.5). The switching of polarization illuminates these subbands and thus makes possible to detect them experimentally.

IV. SUMMARY AND CONCLUSIONS

We investigated quantum states and magneto-optics of 2D holes in a p -type heterojunction subjected to perpendicular magnetic field and periodic potential of surface superlattice. The holes were described by the 4×4 Luttinger Hamiltonian where both confinement potential and potential of lateral surface superlattice have been introduced. This model allowed us to figure out the influence of the spin-orbit coupling onto four-component magnetic Bloch quantum states. We've calculated hole magnetic subbands at high magnetic fields under consideration of several Landau levels originating from the first three subbands of size quantization. In a wider interval of both low and high magnetic fields the set of hole magnetic subbands originating from two coupled Landau levels has been obtained. We found the increasing differences with electron quantum states at high magnetic fields which are caused by the B -dependent off-diagonal terms in the Luttinger Hamiltonian. Then the calculations of matrix elements for transitions between donors and hole magnetic subbands have been performed. We observed the characteristic dependencies of transition intensities on a subband number and the strong dependence on the polarization of luminescence radiation. In particular, at σ^+ (σ^-) polarization the most intensive transitions are to those hole magnetic subbands where "spin"-down(up) components of the wavefunction dominate. The discussed effects allowed us to define the set of parameters (superlattice periods, amplitude of periodic potential and magnetic field) for possible experimental observation of sharp non-overlapping magnetic subbands for 2D holes.

In the following paper we plan to study the magnetotransport properties of laterally modulated 2D hole gas, and, in particular, the quantization of Hall conductance in hole magnetic subbands.

ACKNOWLEDGMENTS

We thank D. Weiss, R.R. Gerhardts and D. Pfannkuche for useful discussions and M. Kohmoto for sending us the offprint of his paper (Ref.9). This work was supported by the RFBR (Grants No. 01-02-17102, 02-02-06440), by the Russian Ministry of Education (Grants No. E00-3.1-413, UR 0101.020) and by the BRHE Program (Project REC - 001).

-
- ¹ J. Zak, Phys. Rev. A **136**, 776, 1647 (1964).
² E.M. Lifshitz and L.P. Pitaevskii, Statistical Physics, Part 2 (Pergamon, New York, 1980).
³ R.E. Peierls, Z.Phys. **80**, 763 (1933).
⁴ D.J. Thouless, M. Kohmoto, M.P. Nightingale, and M. den Nijs, Phys. Rev. Lett. **49**, 405 (1982).
⁵ H. Silberbauer, J. Phys.: Condens. Matter **4**, 7355 (1992).
⁶ D. Pfannkuche and R.R. Gerhardts, Phys. Rev. B **46**, 12606 (1992).
⁷ D. Springsguth, R. Ketzmerick, and T. Geisel, Phys. Rev. B **56**, 2036 (1997).
⁸ V.Ya. Demikhovskii and A.A. Perov, Phys. Low-Dim. Structures **7/8**, 135 (1998).
⁹ M. Kohmoto, Ann. Phys. (NY) **160**, 343 (1985).
¹⁰ N. Usov, Sov. Phys. JETP **67**, 2565 (1988).

- ¹¹ J. Eroms, M. Zitzlsperger, D. Weiss, J.H. Smet, C. Albrecht, R. Fleischmann, M. Behet, J. De Boeck, and G. Borghs, Phys. Rev. B **59**, R7829 (1999).
- ¹² G. Petschel and T. Geisel, Phys. Rev. Lett. **71**, 239 (1993).
- ¹³ R. Ketzmerick, K. Kruse, D. Springsguth, and T. Geisel, Phys. Rev. Lett **84**, 2929 (2000).
- ¹⁴ D. Weiss, P. Grambow, K. von Klitzing, A. Menschig, and G. Weimann, Appl. Phys. Lett. **58**, 2960 (1991).
- ¹⁵ T. Schlösser, K. Ensslin, J. Kotthaus, and M. Holland, Semicond. Sci. Technol. **11**, 1582 (1996); Europhys. Lett. **33**, 683 (1996).
- ¹⁶ C. Albrecht, J.H. Smet, K. von Klitzing, D. Weiss, V. Umansky, and H. Schweizer, Phys. Rev. Lett. **86**, 147 (2001).
- ¹⁷ D. Weiss, *Proc. of the 15th Int. Conf. on High Magnetic Fields in Semicond. Phys.*, Oxford, UK (2002).
- ¹⁸ V.Ya. Demikhovskii and D.V. Khomitskiy, *ibid.*
- ¹⁹ I.V. Kukushkin, D. Weiss, G. Lütjering, R. Bergmann, H. Schweizer, K. von Klitzing, K. Eberl, P. Rotter, M. Suhrke, and U. Rössler, Phys. Rev. Lett. **79**, 1722 (1997).
- ²⁰ O.V. Volkov, V.E. Zhitomirskii, I.V. Kukushkin, W. Dietsche, K. von Klitzing, A. Fischer, and K. Eberl, Phys. Rev. B **56**, 7541 (1997).
- ²¹ J.M. Luttinger, Phys. Rev. **102**, 1030 (1956).
- ²² D.A. Broido and L.J. Sham, Phys. Rev. B **31**, 888 (1985).
- ²³ Yu.A. Bychkov and E.I. Rashba, in the *Proc. of the 17th Int. Conf. on the Phys. Semicond.*, San Francisco (1984), Springer Verlag (1985), p. 321.
- ²⁴ G.E. Marques and L.J. Sham, Surf. Sci. **113**, 131 (1982).
- ²⁵ It should be noted that the particular classification of solutions F_N may be chosen in a different way²⁰ which leads to changes in notation only.
- ²⁶ F. Ancilotto, A. Fasolino, and J.C. Maan, Phys. Rev. B **38**, 1788 (1988).